

Quantifying the effects of non-hydrostatic stress on multi-component minerals

Benjamin L Hess¹, Jay J. Ague¹, and Peter Voorhees²

¹Yale University

²Northwestern University

November 22, 2022

Abstract

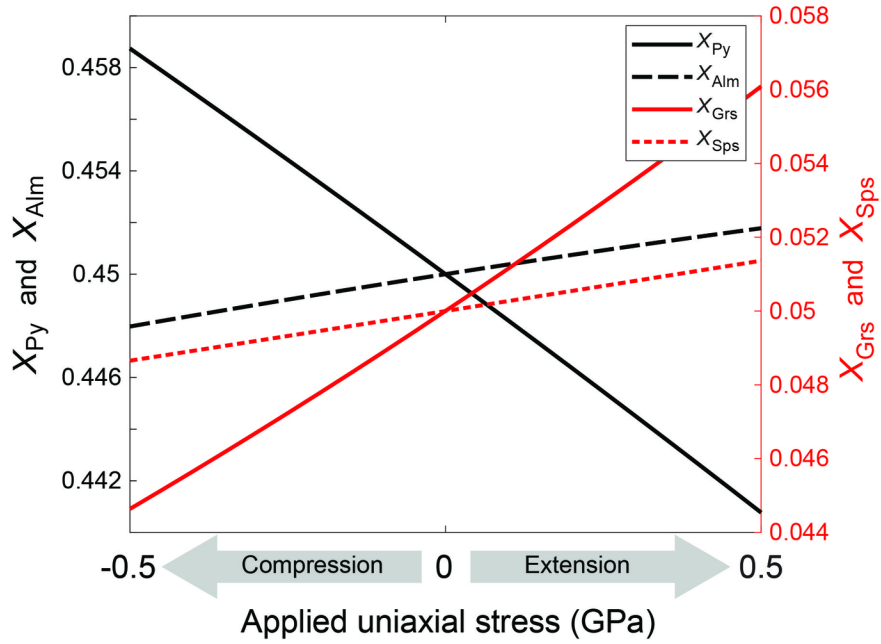
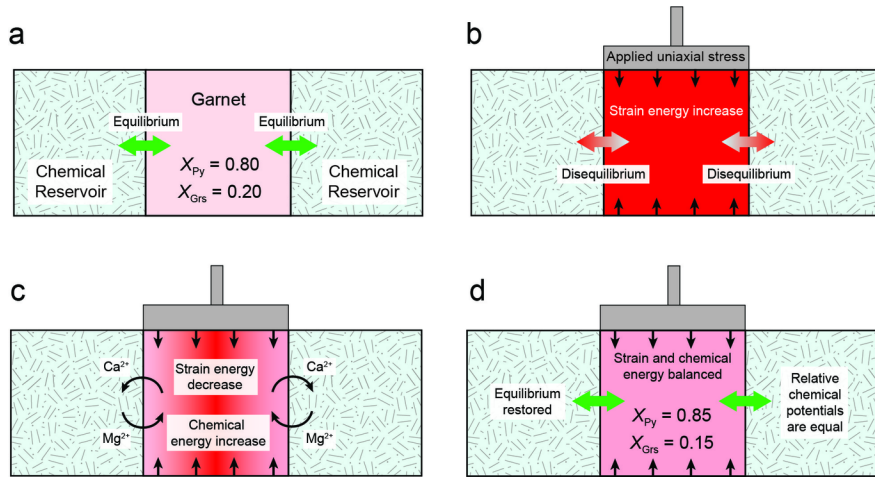
Mineral compositions are used to infer pressures, temperatures, and timescales of geological processes. The thermodynamic techniques underlying these inferences assume a uniform, constant pressure. Nonetheless, convergent margins generate significant non-hydrostatic (unequal) stresses, violating the uniform pressure assumption and creating uncertainty. Materials scientists F. Larché and J. Cahn derived an equation suitable for non-hydrostatically stressed geologic environments that links stress and equilibrium composition in elastic, multi-component crystals. However, previous works have shown that for binary solid solutions with ideal mixing behavior, hundreds of MPa to GPa-level stresses are required to shift mineral compositions by a few hundredths of a mole fraction, limiting the equation's applicability. Here, we apply Larché and Cahn's equation to garnet, clinopyroxene, and plagioclase solid solutions, incorporating for the first time non-ideal mixing behavior and more than two endmembers. We show that non-ideal mixing increases predicted stress-induced composition changes by up to an order of magnitude. Further, incorporating additional solid solution endmembers changes the predicted stress-induced composition shifts of the other endmembers being considered. Finally, we demonstrate that Larché and Cahn's approach yields positive entropy production, a requirement for any real process to occur. Our findings reveal that stresses between tens and a few hundred MPa can shift mineral compositions by several hundredths of a mole fraction. Consequently, mineral compositions could plausibly be used to infer stress states. We suggest that stress-composition effects could develop via intracrystalline diffusion in any high-grade metamorphic setting, but are most likely in hot, dry, and strong rocks such as lower crustal granulites.

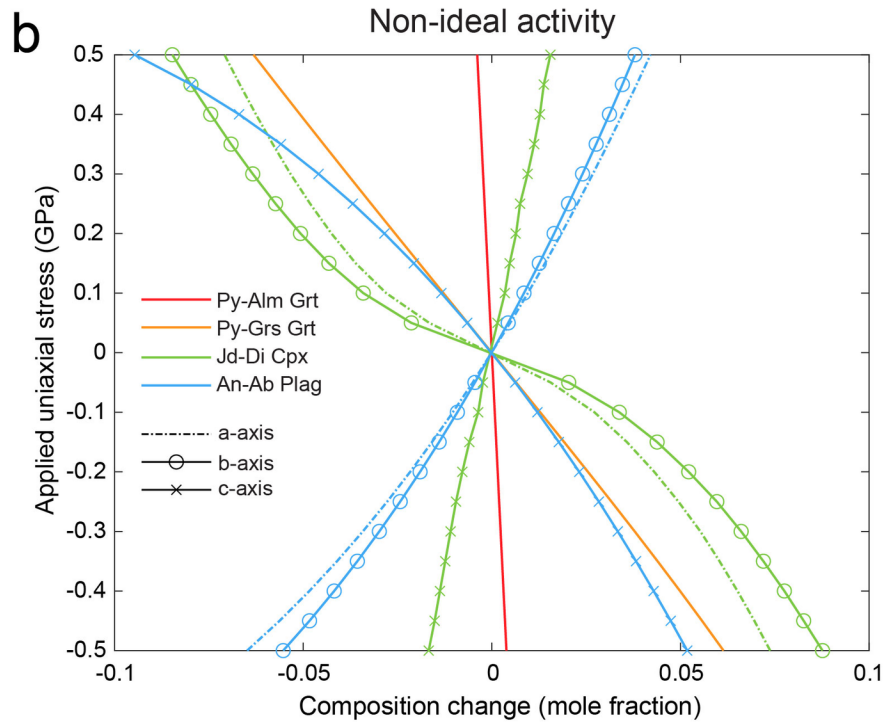
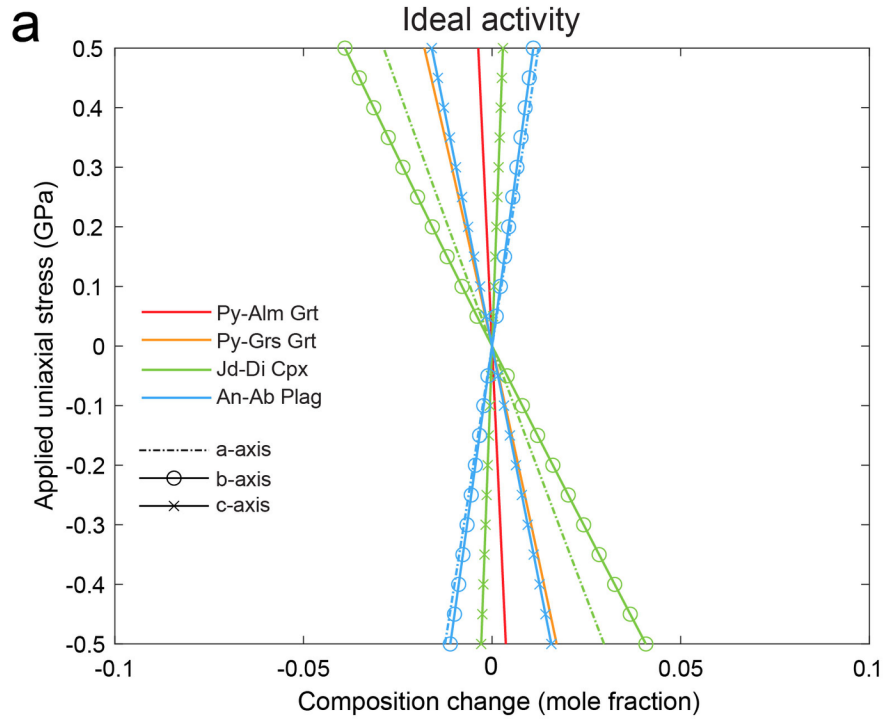
Hosted file

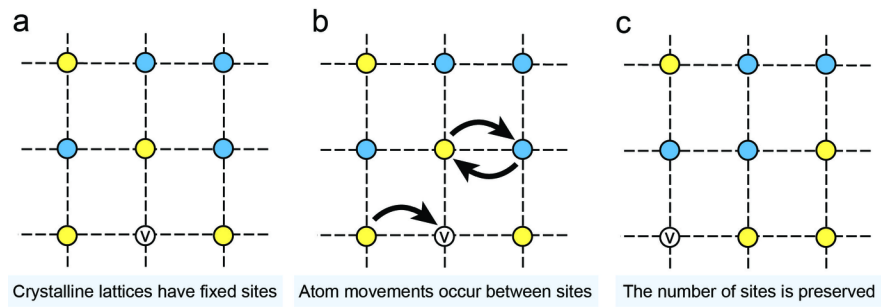
manuscript_revised_suppinfo.docx available at <https://authorea.com/users/535481/articles/598774-quantifying-the-effects-of-non-hydrostatic-stress-on-multi-component-minerals>

Hosted file

essoar.10511970.1.docx available at <https://authorea.com/users/535481/articles/598774-quantifying-the-effects-of-non-hydrostatic-stress-on-multi-component-minerals>







Quantifying the Effects of Non-hydrostatic Stress on Multi-component Minerals

Benjamin L. Hess¹, Jay J. Ague^{1,2}, and Peter W. Voorhees³

¹ Department of Earth and Planetary Sciences, Yale University, PO Box 208109, New Haven, CT 06520-8109, USA.

² Yale Peabody Museum of Natural History, Yale University, New Haven, CT 06511, USA

³ Department of Materials Science and Engineering, Northwestern University, Evanston, IL 60208, USA

Corresponding author: Benjamin Hess (benjamin.hess@yale.edu)

Key Points:

- Non-ideal mixing increases stress-induced composition changes in minerals by up to an order of magnitude compared to ideal mixing.
- All pertinent solid solution endmembers should be considered to determine how stress changes affect the composition of each endmember.
- Stress-induced composition effects are likely to develop in hot, dry rocks comprising strong minerals such as lower crustal granulites.

Abstract

Mineral compositions are used to infer pressures, temperatures, and timescales of geological processes. The thermodynamic techniques underlying these inferences assume a uniform, constant pressure. Nonetheless, convergent margins generate significant non-hydrostatic (unequal) stresses, violating the uniform pressure assumption and creating uncertainty. Materials scientists F. Larché and J. Cahn derived an equation suitable for non-hydrostatically stressed geologic environments that links stress and equilibrium composition in elastic, multi-component crystals. However, previous works have shown that for binary solid solutions with ideal mixing behavior, hundreds of MPa to GPa-level stresses are required to shift mineral compositions by a few hundredths of a mole fraction, limiting the equation's applicability. Here, we apply Larché and Cahn's equation to garnet, clinopyroxene, and plagioclase solid solutions, incorporating for the first time non-ideal mixing behavior and more than two endmembers. We show that non-ideal mixing increases predicted stress-induced composition changes by up to an order of magnitude. Further, incorporating additional solid solution endmembers changes the predicted stress-induced composition shifts of the other endmembers being considered. Finally, we demonstrate that Larché and Cahn's approach yields positive entropy production, a requirement for any real process to occur. Our findings reveal that stresses between tens and a few hundred MPa can shift mineral compositions by several hundredths of a mole fraction. Consequently, mineral compositions could plausibly be used to infer

stress states. We suggest that stress-composition effects could develop via intracrystalline diffusion in any high-grade metamorphic setting, but are most likely in hot, dry, and strong rocks such as lower crustal granulites.

Plain Language Summary

The chemical compositions of many minerals found in rocks are sensitive to the pressure and temperature conditions at which the minerals form. Thus, we can use mineral compositions to deduce the formation conditions of rocks, giving us insights into important geological processes such as the global carbon cycle and continent formation. The techniques we use to determine these conditions assume that pressure is equal in all directions. However, minerals sometimes form in settings where there is significantly more pressure, or stress, in one direction than another due to, for example, colliding tectonic plates. As a result, there is uncertainty as to how to interpret the compositions of such minerals. In this work, we apply a theory developed by materials scientists that provides a way to quantify the expected compositions of different types of minerals based on the directions and magnitudes of stresses. This approach will enable us to use mineral compositions to learn more about the pressure and stress conditions in important geological settings such as within subduction zones and mountain belts.

1. Introduction

Equilibrium thermodynamics provide a powerful tool for studying lithospheric processes. Thermodynamic models such as pseudosections, for example, can be used to make predictions of where metamorphic reactions occur in the Earth. This in turn can be used to model large-scale processes such as element cycling (e.g., Evans & Powell, 2015; Kerrick & Connolly, 2001; Li et al., 2020; Stewart & Ague, 2018) and mantle dynamics (e.g., Holland et al., 2013; Poli & Schmidt, 2002).

However, there is a fundamental concern regarding the role of unequal (or non-hydrostatic) stresses in equilibrium thermodynamic treatments. Elastic solids can support non-hydrostatic stresses, leading to the possibility of unequal stresses at mechanical equilibrium. Gibbs free energy minimization techniques inherent in geothermobarometry and pseudosection modeling are predicated on the assumption that solid stresses are uniform and hydrostatic (i.e., constant pressure) in a system. However, mounting evidence indicates that domains of non-lithostatic pressure may occur in convergent margins (e.g., Chu et al., 2017; Li et al., 2010; Tajčmanová et al., 2015; Vrijmoed & Podladchikov, 2015; Zuzva et al., 2020). Moreover, these margins are also subject to ubiquitous deviatoric stresses on the order of 10s to 100s of MPa (e.g., Gerya, 2015; Molnar & England, 1993; Jamtveit et al., 2019; Schmalholz et al., 2014a; Stüwe & Sandiford, 1994). Some models even suggest deviatoric stresses as much as or exceeding 1 GPa, at least locally (e.g., Babeyko & Sobolev, 2008; Burg & Gerya, 2005; Burov & Yamato, 2008; Gerya, 2015; Schmalholz et al., 2014b).

There has been long-standing discussion regarding the thermodynamic treat-

ment of non-hydrostatically stressed geological systems (e.g., Bruton & Helgeson, 1983; Dahlen, 1992; Green, 1980; Kamb, 1959, 1961; MacDonald, 1957, 1960; Paterson, 1973; Robin, 1978; Verhoogen, 1951). More recently, considerable vigorous and productive debate has focused on the role of non-hydrostatic stress during metamorphism (Connolly, 2009; Hobbs & Ord, 2016, 2017; Moulas et al., 2019a, 2019b; Powell et al., 2018; Tajčmanová et al., 2014, 2015, 2021; Wheeler, 2014, 2018, 2020). This debate is essential to pursue, as non-hydrostatic stress is likely widespread in active tectonic margins.

We posit that since Gibbsian equilibrium thermodynamics underlies many of our petrological techniques, the best way forward is to use a theory that is based solidly on, and is completely consistent with, Gibbs (1878). The derivations of materials scientists Larché and Cahn (1973, 1978a, 1978b, 1982, 1985) provide this framework. This remarkable body of work (referred to as “Larché-Cahn theory” herein) has been used, for example, to explore the effects of stress on mineral interface stability (e.g., Hess & Ague, 2021; Powell et al., 2018; Wheeler, 2014, 2018).

Herein, we focus on how Larché-Cahn theory can be used to calculate compositions of non-hydrostatically stressed, multi-component minerals. Larché and Cahn (1973, 1985) derive a powerful equation (referred to herein as the “Larché-Cahn equation”) that allows for the equilibrium composition of multi-component elastic solids to be calculated as a function of stress. This is illustrated by the recent studies of Powell et al. (2018) and Wheeler (2018), which use the Larché-Cahn equation to calculate expected stress-induced composition changes in minerals. Wheeler (2018) demonstrates that structurally anisotropic minerals will have different compositions depending on their orientations under non-hydrostatic stress. Consequently, variations in mineral compositions could potentially be used to infer the stresses under which they equilibrated. However, both the results of Wheeler (2018) and Powell et al. (2018) indicate that hundreds of MPa to several GPa of applied stress would be needed to induce a few hundredths of a mole fraction shift in the compositions of common minerals such as plagioclase or pyroxene. The necessity of such large stresses raises the question of whether non-hydrostatic stress can have an appreciable effect on metamorphic mineral compositions.

On the other hand, there are important aspects of mineral solid solutions that have not yet been considered. Specifically, works to date assume ideal mixing and model solid solutions with a maximum of only two components. This represents an important gap in knowledge, as many common solid solutions, such as garnet, are highly non-ideal and consist of more than two components. These considerations have been shown to be important in materials science (e.g., King et al., 1991; Larché & Cahn, 1978a; Voorhees & Johnson, 2004), and are likely to be important in minerals as well. Furthermore, because the stress-induced composition changes we consider are achieved via the irreversible process of intracrystalline diffusion, it must be shown that the requirements of negative free energy change and positive entropy production are satisfied in order for the

application of Larché-Cahn theory to be valid.

In this study, we apply the Larché-Cahn equation to mineral solid solutions with non-ideal mixing behaviors and with more than two endmembers for the first time. Our results show that when non-ideal activity is included, the expected stress-induced composition changes can increase by up to an order of magnitude relative to the assumption of ideal mixing behavior. As such, only stresses on the order of tens to a few hundred MPa may be needed to shift compositions by several hundredths of a mole fraction in minerals such as garnet, plagioclase and clinopyroxene. Consequently, the possibility of using mineral compositions to infer stress conditions becomes more plausible. In addition, we show that when more than two endmembers are considered in a solid solution, the expected magnitudes and even the directions of composition change for individual endmembers can vary significantly. As a result, it is critical to consider all major endmembers in a mineral to predict stress-induced composition changes. Finally, we demonstrate that the composition change predicted by Larché-Cahn theory satisfies the requirements of negative free energy change and positive entropy production, as required for any real process.

2. Larché-Cahn theory

The work of Larché and Cahn (1973, 1978a, 1978b, 1982, 1985) has been hailed as “a milestone of 20th century thermodynamics” (Shi et al., 2018). It has been applied successfully to the study of epitaxial thin films (e.g., Guyer & Voorhees, 1996; Lian et al., 2021; Spencer et al., 1991; Wang et al., 2006), lithium ion batteries (e.g., Bower et al., 2011; Cui et al., 2012; Meca et al., 2016; Sethuraman et al., 2010; Shi et al., 2018), and coherent precipitates in alloys (e.g., Kamachali et al., 2014, 2018; Schwarze et al., 2017; Voorhees & Johnson, 1989). Here we briefly review the key concepts that underlie our work, noting that other recent studies also discuss these concepts from a variety of perspectives (e.g., Powell et al., 2018, 2019; Voorhees & Johnson, 2004; Wheeler, 2018).

Larché and Cahn provide a precise definition for a solid via their network model, which requires a solid to have a definite structure with discrete sites (e.g., a crystal lattice). The network can be modified at interfaces through dissolution and precipitation or at dislocations. Otherwise, the network is constant and exists regardless of the species occupying individual network sites (Fig. 1). For example, the 8-fold coordinated sites in the crystalline structure of a garnet exist whether they are occupied by Fe^{2+} , Mg^{2+} , etc.

The network holds that for a solid with N substitutional species, only $N - 1$ species are independent. For example, in a binary solid, if one species is removed from a lattice site, in order to preserve the lattice network, it must be replaced by another species or a vacancy (Fig. 1b). Therefore, when mole fractions of $N - 1$ species are defined, the mole fraction of the N^{th} species is determined. The N^{th} species is arbitrarily chosen and is termed the “dependent” species. Additional charge balance considerations must also be made for ionic solids. Since there are only $N - 1$ independent species in a multi-component solid, the

number of moles of one species cannot be varied without also changing the number of moles of at least one other species. Consequently, Larché and Cahn (1973, 1978b, 1985) define a new thermodynamic potential for solids that incorporates this additional compositional constraint. We refer to this thermodynamic potential as “relative chemical potential” after Gurtin et al. (2010). Relative chemical potential defines the change in energy resulting from the exchange of one species in a solid with another. The relative chemical potential has also been called the diffusion potential (Larché & Cahn, 1985, with symbol M), the chemical potential of exchange endmembers (Powell et al., 2018), or the chemical potential of an exchange vector (Wheeler, 2018).

As an example, suppose two garnets are composed of pyrope and almandine and are hydrostatically stressed. If the garnets exchange components via diffusion (e.g., pyrope for almandine), then the energy change in that exchange can be defined by the difference in chemical potentials of the endmembers:

$$\mu_{Py-Alm} = \mu_{Py} - \mu_{Alm}$$

where μ_{Py-Alm} is the relative chemical potential defined by the change in energy resulting from adding pyrope (Py) and removing almandine (Alm) in a garnet, and μ is the Gibbsian chemical potential of either pyrope or almandine. Note, however, that when minerals are non-hydrostatically stressed, relative chemical potential is not in general equal to the difference in endmember chemical potentials (Larché & Cahn, 1973, 1985) because chemical potential cannot be used to define equilibrium within non-hydrostatically stressed solids (Gibbs, 1878; Hess & Ague, 2021; Kamb, 1961; Wheeler, 2018).

Using the network model and relative chemical potential, Larché and Cahn (1973, 1978b) employ the same variational calculus approach of Gibbs (1878) to derive general equilibrium conditions for multi-component, elastic solids under non-hydrostatic stress. They show that the interior of a non-hydrostatically stressed multi-component solid is at chemical equilibrium when all relative chemical potentials are uniform. The requirement of uniform relative chemical potentials indicates that chemical equilibrium is achieved when the overall system energy cannot be reduced by further *exchange* of species between the solid and the surrounding system or within the solid itself. Additionally, when the stress state is hydrostatic, the relative chemical potentials in a solid simplify to the differences in Gibbsian chemical potentials (Larché & Cahn, 1985) and the classical equilibrium conditions derived by Gibbs (1878) are recovered.

3. Methods

3.1. The Larché-Cahn equation

From their equilibrium conditions, Larché and Cahn (1973, 1985) define a new Maxwell relationship that applies to relative chemical potential. The detailed steps of how they arrive at this relationship are given by Voorhees and Johnson (2004). The relationship is (after Larché & Cahn, 1985, eq. 4.13):

$$\left(\frac{\partial\mu_{I-K}}{\partial\sigma_{ij}}\right)_{X,\sigma_{kl}\neq ij} = -V_0 \left(\frac{\partial\varepsilon_{ij}}{\partial X_{I-K}}\right)_{X_{J\neq I,K},\sigma_{ij}} \#(1)$$
 where μ_{I-K} is the relative chemical potential between species I and dependent species K (J mol⁻¹), σ_{ij} is the stress tensor (Pa) where ij follows indicial notation, X is mole fraction, V_0 is the molar volume of the solid in at the reference pressure and temperature (m³ mol⁻¹), ε_{ij} is the strain tensor, X_{I-K} is the mole fraction of I assuming dependent species K, and X_J is the mole fraction of all other independent species which are not I or K.

Equation (1) relates stress, strain, composition, and relative chemical potential in multi-component minerals. To use it quantitatively, Larché and Cahn (1973) apply Hooke’s Law of linear elasticity and integrate the resulting expression from a reference pressure to a stress of interest along a constant temperature and composition path (after Larché & Cahn, 1985):

$$\mu_{I-K}(\sigma_{ij}, X_{I-K}) = \mu_I^*(P) - \mu_K^*(P) + RT \ln\left(\frac{a_I}{a_K}\right) - V_0 \frac{\partial\varepsilon_{ij}^c}{\partial X_{I-K}} (\sigma_{ij} + P\delta_{ij}) - \frac{V_0}{2} \frac{\partial S_{ijkl}}{\partial X_{I-K}} (\sigma_{ij}\sigma_{kl} - P^2\delta_{ij}\delta_{kl}) \#(2)$$

where $\mu_{I-K}(\sigma_{ij}, X_{I-K})$ is the relative chemical potential (J mol⁻¹) between independent species I and dependent species K at given stress, σ_{ij} , and composition, X_{I-K} ; $\mu^*(P)$ is the Gibbsian chemical potential (J mol⁻¹) of pure species I or K defined at a reference pressure, P (Pa), and temperature, T (K); R is the ideal gas constant (J mol⁻¹ K⁻¹); a is the activity of species I or K; V_0 is the molar volume of the solid in at the reference pressure and temperature (m³ mol⁻¹); ε_{ij}^c is the composition strain (unitless); δ_{ij} is the Kronecker delta; and S_{ijkl} is the compliance tensor (Pa⁻¹).

Equation (2) (the ‘‘Larché-Cahn equation’’) is a powerful result that allows for the calculation of equilibrium compositions and stresses in non-hydrostatically stressed minerals. It can be used to both calculate expected compositions given applied stresses (as we do in this work), and, in future applications, calculate stresses given measured mineral compositions.

The Larché-Cahn equation is fully and readily solvable given the wealth of available data for mineral thermodynamic properties (e.g., Green et al., 2016; Holland et al., 2021; Holland & Powell, 2011; White et al., 2014) and material properties (e.g., Brown et al., 2016; Holland & Powell, 2011; Zhao et al., 1997, 1998). The chemical potential terms are defined using standard Gibbs free energy calculations at any desired reference pressure and temperature (e.g., Holland & Powell, 2011), and activities are calculated using known activity models. The tensor that describes the change in strain energy with composition change, $\frac{\partial\varepsilon_{ij}^c}{\partial X_{I-K}}$ (denoted ε_{ij} by Larché and Cahn (1985)), can be determined from known crystal lattice parameters. Wheeler (2018) refers to this tensor as ‘‘partial molar strain’’ and provides a thorough exposition for calculating it in Appendix S3 of the same work. Additionally, simplifications can often be made to the

Larché-Cahn equation such as assuming that the elastic constants do not vary with composition. This assumption is often valid to first order, and we make it in the remainder of this paper for simplicity. As a consequence, the last term in equation (2) drops out, and the Larché-Cahn equation simplifies to:

$$\mu_{I-K}(\sigma_{ij}, X_{I-K}) = \mu_I^*(P) - \mu_K^*(P) + RT \ln\left(\frac{a_I}{a_K}\right) - V_0 \eta_{ij}^{I-K} (\sigma_{ij} + P\delta_{ij}) \quad \#(3)$$

noting that η_{ij}^{I-K} has now replaced $\frac{\partial \varepsilon_{ij}^c}{\partial X_{I-K}}$.

3.2. Solving the Larché-Cahn equation

Herein, we are primarily interested in showing how composition can be calculated given a specific stress tensor. Therefore, we will assume that the reference pressure and the final stress tensor are defined variables. To determine the direction and magnitude of the effect of stress on the composition, we hold the relative chemical potentials of the system constant. However, we note that since the relative chemical potential is a state function, it need not be fixed in a natural system. Choosing to hold the relative chemical potential constant, therefore, is simply a matter of convenience for our analysis. By fixing the relative chemical potential, we can use the Larché-Cahn equation to numerically determine the composition as a function of stress.

Solving the Larché-Cahn equation is relatively straightforward for ideal binary solid solutions (e.g., Larché & Cahn, 1985; Powell et al., 2018; Wheeler, 2018). For a specified stress state, reference pressure, and relative chemical potential, the composition that satisfies equation (3) is the solution. Here, however, we consider non-ideal mixing behavior which adds additional complexity. An activity model must be used to transform compositions to activities in order to find the composition that satisfies equation (3). Example calculations for two non-ideal binary solid solutions are provided in Supporting Information S1.

In addition, we also consider solid solutions with more than two endmembers for the first time. For each additional endmember, another relative chemical potential must be defined. This means that the Larché-Cahn equation must be solved for each relative chemical potential simultaneously, defining a system of equations. Finding the composition and corresponding activities that then satisfies all equations is not trivial and typically requires an optimization method. We employ maximum likelihood estimation (e.g., Myung, 2003) to find the mineral composition that satisfies all relative chemical potentials simultaneously.

4. Results

The results of this section predict how the composition of mineral grains change with applied stress relative to a hydrostatic reference pressure.

4.1. Illustrative example

One method for solving equation (3) is to stipulate that the relative chemical potentials of the surroundings are constant. This applies, for example, when the surroundings are sufficiently large and homogeneous such that diffusive exchange between the stressed mineral and the surroundings will not significantly alter the relative chemical potentials of the surroundings. In this way, the surroundings act as a chemical reservoir. A chemical reservoir could take the form of other minerals in the rock matrix, intergranular films, or fluids. In dry systems, structural impediments to interface motion (e.g., the movement of steps at solid-solid interfaces) would allow for diffusion through grain boundaries (and thus uniform relative chemical potentials) without interface migration. If present, however, fluids are more likely to drive interface evolution which is discussed in section 5.4. But for simplicity, the interfaces are assumed to be stationary in our first example which is schematic and intended only to illustrate how stress and composition interact (Fig. 2).

Let us consider a garnet composed only of pyrope and grossular that is hydrostatically stressed and in equilibrium with a chemical reservoir that fixes the relative chemical potentials of the system (Fig. 2a). Suppose that a compressive uniaxial stress is uniformly applied to the entire garnet (Fig. 2b). The relative chemical potential increases because the stress adds strain energy to the garnet. But since the surroundings have fixed relative chemical potentials, the garnet can reduce the strain energy by exchanging the larger grossular component for the smaller pyrope component via diffusion (Fig. 2c). The tendency for species with smaller volumes to diffuse toward regions of higher compressive stress to reduce strain energy is an oft-cited phenomenon referred to as the Gorsky effect (Gorsky, 1935). The Gorsky effect is commonly observed, for example, in interstitial hydrogen diffusion in stressed alloys (e.g., Fukai et al., 1985; Pálsson et al., 2012; Schaumann et al., 1968, 1970; Shi et al., 2018; Völkl, 1972). Equation (3) indicates that this diffusive exchange will occur until the decrease in strain energy exactly balances the increase in chemical energy. At this point, the relative chemical potential between pyrope and grossular is once more equal to the relative chemical potential of the surroundings (Fig. 2d).

Quantitatively, for example, let the initial garnet composition be $X_{\text{Py}} = 0.8$, the temperature be 600 °C, and the pressure be 1 GPa (Fig. 2a). Let us assume that the final applied stress is -0.5 GPa (a negative stress is compressive by convention; Fig. 2b). Assuming that the relative chemical potential remains constant, we solve equation (3) to find that the new composition of the garnet is $X_{\text{Py}} = 0.851$ (Fig. 2d). Supporting Information S1 provides a detailed solution of this problem.

4.2. Composition changes in binary solid solutions

Using the same logic of a chemical reservoir, we solve equation (3) assuming a fixed relative chemical potential for four common metamorphic mineral binary solid solutions: pyrope-almandine (Py-Alm) and pyrope-grossular (Py-Grs) in garnet, jadeite-diopside (Jd-Di) in clinopyroxene, and anorthite-albite (An-Ab) in plagioclase (Fig. 3). We have incorporated structural anisotropy and consider

both ideal solid solution mixing (Fig. 3a) and non-ideal mixing (Fig. 3b).

For ideal mixing, the Py–Grs binary has a significantly larger composition change as a function of stress than does the Py–Alm binary (Fig. 3a). This results from the larger molar volume difference between Py–Grs endmembers than between Py–Alm. The difference in stress-induced composition changes between the two binaries becomes more pronounced when non-ideal mixing behavior is considered. While the Py–Alm solid solution is nearly ideal, the Py–Grs solid solution is highly non-ideal (Berman, 1990; Ganguly et al., 1996; White et al., 2014). Thus, the Py–Alm binary composition change remains virtually the same compared to the ideal case whereas the Py–Grs composition change increases by a factor of about 3.5 compared to the ideal case (Fig. 3b). Non-ideal mixing likewise increases the predicted composition change by up to 5 to 10 times for the Jd–Di and An–Ab binaries, respectively, compared to assuming ideal mixing.

In addition to molar volume differences and mixing behaviors, crystal symmetry is important (Wheeler, 2018). As garnet is an isotropic mineral, it does not matter which axis stress is applied to; the predicted composition change is the same regardless. In contrast, clinopyroxene and plagioclase are structurally anisotropic. Consequently, the predicted composition change depends on which crystallographic axis stress is applied to for the Jd–Di and An–Ab solid solutions. For example, stress applied to the b -axis of omphacite leads to a greater increase in X_{Jd} compared to the a -axis. In addition, different axes can even lead to opposite directions of composition change. For example, if stress is applied to the c -axis of omphacite, X_{Jd} will decrease.

4.3. Composition change in ternary and higher solid solutions

The Larché-Cahn equation can be used to determine the composition in solid solutions with an arbitrary number of components if the stress state and relative chemical potentials are specified. When there are more than two components, a relative chemical potential must be defined for each independent endmember and the arbitrarily chosen dependent endmember. For example, if the common garnet quaternary system pyrope–almandine–grossular–spessartine (Py–Alm–Grs–Sps) is considered, then there will be three relative chemical potentials between three of the endmembers and the chosen fourth endmember. For any given stress state, the composition that satisfies all of the relative chemical potential values simultaneously is the equilibrium composition.

Here we show the resulting composition change in a garnet with a reference composition of $X_{\text{Py}} = X_{\text{Alm}} = 0.45$ and $X_{\text{Grs}} = X_{\text{Sps}} = 0.05$ and reference conditions of 1 GPa and 600 °C (Fig. 4). As compressive stress is applied, X_{Py} increases while X_{Alm} , X_{Grs} , and X_{Sps} decrease. The trends are opposite for extensional stress. The composition change is greatest for the Py and Grs components as they have the largest molar volume difference and the most non-ideal mixing behavior (Holland & Powell, 2011; White et al., 2014).

5. Discussion

By examining the change between a reference pressure and a final stress state, we are able to make predictions about the compositions of minerals under non-hydrostatic stress (Fig. 2–4). Our results build on the previous work of Powell et al. (2018) and Wheeler (2018) in important ways by incorporating not only structural anisotropy, but for the first time, non-ideal mixing and solid solutions with more than two endmembers. Considering non-ideal mixing behavior can give rise to significantly larger stress-induced compositional shifts compared to the assumption of ideal mixing. Further, including additional endmembers in a solid solution can change both the predicted magnitude and even direction of composition change in each individual endmember. Consequently, incorporating both non-ideal mixing and all major endmembers in a solid solution is essential for modeling stress-induced composition changes.

5.1. Effects of non-ideal mixing

Powell et al. (2018) and Wheeler (2018) have used the Larché-Cahn equation with constant relative chemical potential to predict composition changes in ideal binary solid solutions. When ideal mixing behavior is assumed, the difference in expected composition changes between different solid solution binaries is due solely to the difference in endmember molar volumes for isotropic solids and unit cell dimensions for anisotropic solids (Fig. 3a). Powell et al. (2018), for example, calculate the expected composition change in plagioclase feldspar assuming it to be both isotropic and ideal at a reference temperature of 650 °C and 0.8 GPa. They find that by increasing the mean stress by 330 MPa (i.e., adding 330 MPa to the three principal stresses), the expected composition change is 0.0035 mole fraction. Wheeler (2018) arrives at a comparable result. At 500 °C and atmospheric pressure, Wheeler calculates that a 2 GPa increase in mean stress is required to change the mole fraction of plagioclase by 0.02.

However, solid solutions that have large molar volumes differences typically also have highly non-ideal behavior such as the garnet, plagioclase, and clinopyroxene solid solutions we consider here (Green et al., 2016; Holland & Powell, 2003; White et al., 2014). Considering non-ideality can thus have substantially larger effects than the difference in unit cell dimensions (Fig. 3b). Non-ideal mixing with positive deviations from ideality (as is the case for the solid solutions considered in this work) acts to decrease the change in chemical energy with composition change. Thus, additional composition change is required to balance the imposed strain energy from an applied stress compared to the assumption of ideality.

The effects of non-ideal mixing increase the expected composition change by up to an order of magnitude depending on how close the composition is to a solvus (Larché & Cahn, 1978a, 1985). For example, the Jd–Di binary at 750 °C with a composition of $X_{\text{Jd}} = 0.37$ is near a solvus (Green et al., 2016). Consequently, when non-ideal mixing is incorporated, the predicted change in X_{Jd} with applied stress near the solvus is approximately 5 times greater than predicted when ideal mixing behavior is assumed. Thus, for binaries such as in omphacite and plagioclase which have highly non-ideal behavior, incorporating

these effects is important, especially for compositions near a solvus.

5.2. Effects of structural anisotropy

Crystallographic symmetry determines the strain energy imparted by non-hydrostatic stress as a function of orientation. For cubic minerals such as garnet, the orientation of the mineral in a stress field does not matter; the amount of strain imparted by an applied stress will always be the same. Thus, Fig. 3 need not specify to which axis the stress is applied. This also means that applying 300 MPa stress to one crystallographic axis of a garnet adds the same strain energy as applying 100 MPa to all three axes. Consequently, the equilibrium composition of an isotropic mineral is a function of the mean stress. This means that the strain energy of a non-hydrostatically stressed isotropic mineral is equivalent to the strain energy of the same mineral at a hydrostatic stress equal to the mean stress. Since under hydrostatic stress the relative chemical potential of a solid is equivalent to the difference in endmember chemical potentials, the relative chemical potential of an isotropic solid under non-hydrostatic stress is always equal to the difference in chemical potentials of the endmembers (i.e., $\mu_{I-K} = \mu_I - \mu_K$) defined at a pressure equal to the mean stress (Larché & Cahn, 1985). However, this is not generally true for anisotropic minerals.

When a structurally anisotropic mineral is considered (e.g., clinopyroxene or plagioclase), mineral orientation can have an appreciable effect on expected composition change and relative chemical potential. For example, Wheeler (2018) incorporates structural anisotropy and shows that if a change in stress is applied to only one axis of plagioclase, the expected composition change is significantly larger compared to when stress is applied uniformly to all crystallographic axes. The substantial difference is due to the opposite slope directions of the a - and b -axes compared to the c -axis; when stress is applied equally to all three axes, the predicted increase in X_{An} from the c -axis competes against the decrease in X_{An} from the a - and b -axes, resulting in a considerably more modest change than a uniaxial stress applied to any one axis predicts (Fig. 3). We show that a similar behavior is predicted in the Jd-Di binary (Fig. 3; Zhao et al., 1997, 1998). Thus, for both omphacite and plagioclase, non-hydrostatic stress could either increase or decrease the composition, depending on the mineral orientation.

Composition being a function of orientation has two important implications. First, this indicates that the mean stress cannot be used to determine the composition of anisotropic minerals under stress. Likewise, the relative chemical potential is no longer equal to the difference in endmember chemical potentials at a pressure equal to the mean stress since orientation must also be considered (i.e., $\mu_{I-K} \neq \mu_I - \mu_K$). Second, Wheeler (2018) notes that composition differences between solid solution minerals in equilibrium could be used to infer the stresses under which they equilibrated (i.e., be used as “paleopiezometers”). As such, if the compositions and orientations of many mineral grains are known, equation (3) could be used to calculate the stress. Consequently, this would allow for a novel type of geobarometer wherein a single type of mineral (e.g.,

omphacite or plagioclase) could be used to calculate not only a pressure value, but the true principal stress values.

Previous studies demonstrated that when ideal mixing behavior is assumed, stresses on the order of hundreds of MPa to several GPa are required to shift compositions by a few hundredths of a mole fraction (Fig. 3a; Powell et al., 2018; Wheeler, 2018). But we have shown that incorporating non-ideal mixing behavior increases those predicted magnitudes by up to an order of magnitude (Fig. 3b). Consequently, more modest stresses of tens to a few hundred MPa are predicted to shift compositions by several hundredths of a mole fraction (Fig. 3b). Such variations are measurable via electron-probe microanalysis and therefore may have practical applications.

5.3. Ternary and higher solid solutions

For binary solid solutions, composition increase or decrease with applied stress can be qualitatively predicted just by considering the relative lattice dimensions of the endmembers. For example, almandine garnet has a smaller molar volume than grossular, and consequently, X_{Alm} will increase with increasing compressive stress. This phenomenon is known as the Gorsky effect (Gorsky, 1935), and occurs because a mineral’s strain energy is relieved when larger components are exchanged for smaller components in a stressed region. Consequently, in heterogeneously stressed minerals such as garnet, for example, smaller components such as pyrope will preferentially diffuse toward higher stress regions while larger components such as grossular will diffuse toward lower stress regions (Fig. 3). It is possible that such patterns might be observed, for example, around stressed inclusions in garnets.

While the Gorsky effect holds true in general, how each endmember behaves can be less intuitive when additional endmembers are considered. We present results for the first time of stress-induced composition changes in a solid solution with more than two endmembers (Fig. 4). Our results indicate that when additional endmembers are included, the predicted magnitude and even direction of each endmember concentration can change. The changes in predicted compositions occur because the lattice parameters and mixing behaviors of all endmembers must interact to satisfy all relative chemical potentials within the mineral.

In the Py–Alm–Grs–Sps garnet solid solution, for example, pyrope, almandine, and spessartine have similar molar volumes whereas grossular has a significantly larger molar volume. One might expect then that with an increase in compressive stress, X_{Py} , X_{Alm} , and X_{Sps} would all increase and X_{Grs} would decrease. Yet, at the conditions given in Fig. 4, only X_{Py} increases while the mole fractions of the other three endmembers decrease. Pyrope and grossular have the largest changes in mole fraction as they have highly non-ideal mixing behavior (White et al., 2014) and the largest molar volume difference. Therefore, they experience the largest composition shifts under an applied stress (Fig. 4), consistent with the Gorsky effect.

However, the composition changes of almandine and spessartine fall between

pyrope and grossular because they behave relatively ideally with all endmembers (White et al., 2014) and have molar volumes between pyrope and grossular (Holland & Powell, 2011). Whether almandine and spessartine mole fractions increase or decrease with applied stress can vary depending on the bulk composition and temperature. For example, for more almandine-rich garnets, almandine can increase with applied stress. Consequently, it is important to model all pertinent endmembers when determining stress-induced composition changes.

5.4. Preservation of stress-induced composition changes

Our results predict the internal composition that would minimize the free energy within an isotropic or anisotropic multi-component mineral under non-hydrostatic stress. Any non-hydrostatically stressed multi-component mineral could potentially record these stress-composition effects. However, whether they develop and are preserved is dependent on factors such as diffusion rates, the presence or absence of fluids, and deformation.

5.4.1. Diffusion rates, fluids, and deformation

If minerals are subject to a change in stress regime, intracrystalline diffusion rates will determine whether stress-induced composition change will occur. Thus, these effects are most likely to be seen where diffusion is comparatively fast. For the minerals discussed here (garnet, omphacite, and plagioclase), this will be in higher grade metamorphic settings that have temperatures sufficient to facilitate appreciable intracrystalline diffusion. If there is insufficient time for mineral grains to achieve their equilibrium compositions, frozen chemical diffusion profiles with a few hundredths of mole fraction variation would be observed. Such stress-induced diffusion profiles could also be examined and offer not only insights about stress, but also time scales.

However, when considering the development and preservation of stress-induced composition changes, we must also examine the possible role of fluids and deformation. Fluid-driven processes such as pressure solution (e.g., Alcantar et al., 2003; Bernabé & Evans, 2014; Gratier, 1987; Lehner, 1990; Rutter, 1983) and interface-coupled dissolution-precipitation reactions (ICDR; e.g., Ague & Axler, 2016; Centrella et al., 2015; Harlov et al., 2011; Putnis, 2002; Putnis & Austrheim, 2010; Putnis & John, 2010; Wintsch & Yi, 2002) could diminish or remove any stress-induced compositional effects. While pressure solution is a fundamentally important stress-driven mechanism, it is typically most prevalent in the upper crust (Gratier et al., 2013; Lehner, 1990). Consequently, it is less of a consideration at the higher metamorphic grades we consider here, although exceptions are certainly observed (e.g., Smitt et al., 2011).

The process of ICDR, however, is common at higher metamorphic grades and could eliminate slower diffusional stress-induced composition changes. When infiltrating fluids are out of chemical equilibrium with a given mineral in a rock, the fluids will tend to dissolve the mineral and replace it with a new phase or phases with compositions dictated by the fluid chemistry. Nevertheless, there are many cases where ICDR only partially replaces minerals (e.g., Ague & Axler,

2016; Altree-Williams et al., 2015; Engvik et al., 2009; Geisler et al., 2007; Keller & Ague, 2018; Plümper & Putnis, 2009; Rubatto et al., 2008), meaning that the unreacted regions may still preserve stress-induced composition effects. Thus, we suggest that stress-induced compositional variations could potentially be preserved in environments where fluid-mediated dissolution and precipitation operate, although it may be less probable.

In addition to fluid-mediated processes, non-hydrostatic stress at high metamorphic grades can lead to crystal plastic deformation. However, studies have shown that the minerals we consider (garnet, omphacite, and plagioclase) are exceptionally strong, especially when dry (e.g., Bystricky & Mackwell, 2001; Dimanov et al., 1999; Karato et al., 1995; Li et al., 2006; Mei et al., 2010; Rybacki & Dresen, 2004; Wang & Ji, 1999; Zhang & Green, 2007). Consequently, these minerals are likely able to sustain non-hydrostatic stresses at high metamorphic temperatures (e.g., 500-800 °C) with limited deformation. The strength of these minerals increases the likelihood that stress-induced composition effects would be preserved.

When fluids are absent (i.e., the rocks are dry) and the temperature is sufficiently high, the types of stress-induced composition effects we calculate are more likely to develop (Section 5.4.2). Nonetheless, we propose that while fluids and deformation may act to eliminate stress-induced composition effects, in many cases they may be partially preserved due to incomplete fluid-mediated reactions and/or mineral strength.

5.4.2. Dry systems and the lower crust

Hot, dry rock comprising strong minerals such as lower crustal granulites offer an ideal environment to test and apply our predictions. There are many examples of exhumed dry lower crustal granulite facies rocks such as in the Lindås Nappe, Norway, (e.g., Austrheim, 1987, 2013; Jamtveit et al., 2019; Petley-Ragan et al., 2018; Putnis et al., 2017), the Athabasca granulite terrane (Orlandini et al., 2019; Regan et al., 2014), Lofoten, Norway (e.g., Campbell et al., 2020; Jamtveit et al., 2019; Menegon et al., 2021), the Musgraves Range, Australia (Camacho et al., 1995; Menegon et al., 2021), and the Calabria Terrane, Italy (Altenberger et al., 2013). These granulites all preserve pseudotachylites formed by brittle failure, indicating that these rocks were extremely strong and resistant to crystal plastic deformation. Brittle failure of granulite is thought to be a mechanism for hydrating and weakening initially strong crust in orogenic wedges (e.g., Austrheim, 2013; Jamtveit et al., 2019; Menegon et al., 2021; Petley-Ragan et al., 2018). Consequently, there is great interest in understanding the stress states in the lower crust and the role that they play in crustal rheology and plate tectonics (Menegon et al., 2021). However, techniques that can quantify the such stresses are limited.

We propose that these rocks are promising candidates for testing and applying our predictions. They are dry, and the presence of pseudotachylites suggests that they sustained hundreds of MPa or more of differential stresses (e.g., Camp-

bell et al., 2020; Jamtveit et al., 2019; Menegon et al., 2021). Additionally, they are at temperatures that allow for appreciable intracrystalline diffusion, and they often contain the same minerals that we model in this study (garnet, plagioclase, and pyroxene). Stress-induced compositional effects would be best preserved in granulites that were exhumed relatively rapidly (e.g., Granulitgebirge Massif, Germany; Müller et al., 2015). Being able to constrain the stress states in deep granulitic rocks would provide valuable insights into the evolution of lower crustal rocks prior to and during subduction and ultimate continental amalgamation. Consequently, Larché-Cahn theory could be used to provide constraints for important geodynamic models and tectonic processes.

6. Free energy imbalance and entropy production

The Larché-Cahn equation assumes that the interior of a multi-component solid will tend toward uniform relative chemical potentials, as this satisfies the variational calculus used to derive Larché and Cahn’s (1973) equilibrium conditions. However, the process by which equilibrium is satisfied (i.e., diffusion) is an irreversible process. For an irreversible process such as diffusion to occur under isothermal conditions, the free energy change must be negative, and the entropy production must be positive.

For a substitutional crystalline solid undergoing simultaneous deformation and chemical diffusion in an isothermal system with constant composition, the Helmholtz free energy imbalance can be modeled as follows (after Gurtin et al., 2010, eq. 65.9 and p. 406):

$\dot{\psi}_R - \mathbf{T}_R \bullet \dot{\mathbf{F}} + \mathbf{h}_R \bullet \nabla \mu_{I-K} \leq 0$ (4) where ψ is the Helmholtz free energy (J mol⁻¹), \mathbf{T} is the Piola stress tensor (Pa m³ mol⁻¹), \mathbf{F} is the deformation gradient tensor (dimensionless), \mathbf{h} is the vector of species flux per unit area, μ_{I-K} is the relative chemical potential between species I and K (J mol⁻¹), the accent dot represents the time derivative, and the subscript R indicates the material (Lagrangian) frame.

The free energy imbalance expression follows from the definition of Helmholtz free energy $\psi \equiv E - TS$, where E is internal energy, T is absolute temperature, and S is entropy. The second term on the left-hand side of Eq. (4) represents the temporal evolution of internal energy in the deforming solid, and the third term is the product of T and the entropy production due to diffusion in the solid. The species flux term, \mathbf{h}_R , in equation (4) can be replaced with Fick’s law of diffusion written in terms of relative chemical potential (after Gurtin et al., 2010, equation 72.25): $\mathbf{h}_R = -\mathbf{M}_R \nabla \mu_{I-K}$ (5) where \mathbf{M} is the mobility tensor, which is isotropic (a scalar) for the case of cubic symmetry. The negative sign in front of \mathbf{M}_R indicates that diffusion occurs from high to low relative chemical potentials. Substitution of equation (5) with isotropic mobility (M_R) into equation (4) yields the following free energy imbalance expression required for a real process to occur

$$\dot{\psi}_R - \mathbf{T}_R \bullet \dot{\mathbf{F}} + (-M_R |\nabla(\mu_{I-K})|^2) \leq 0 \#(6)$$

where $|\nabla(\mu_{I-K})|$ is the vector magnitude of $\nabla(\mu_{I-K})$.

The third term in equation (6) is the product of the entropy production and T ; consequently, we can isolate this term to show that entropy production is positive, for example, for a binary isotropic solid. For this case, we can replace the relative chemical potential with the difference in molar chemical potentials of the two endmembers defined at the mean stress (see section 5.2). Thus:

$$|\nabla(\mu_{I-K})|^2 = \nabla(\mu_I - \mu_K) \bullet \nabla(\mu_I - \mu_K) = |\nabla(\mu_I - \mu_K)|^2$$

which yields

$$T\dot{S}_R = M_R |\nabla(\mu_I - \mu_K)|^2$$

As a consequence, the entropy production can be written as

$$\dot{S}_R = \frac{M_R |\nabla(\mu_I - \mu_K)|^2}{T} \#(7)$$

Because $M_R \geq 0$, $T \geq 0$, and $|\nabla(\mu_I - \mu_K)|^2 \geq 0$, equation (7) shows that the entropy production is greater than or equal to zero, as required by the Second Law of Thermodynamics. Nonetheless, a recent analysis states that Larché-Cahn theory can give rise to negative entropy production (Tajčmanová et al., 2021). However, their analysis uses the barycentric formulation (J kg^{-1}) for the chemical potentials in equation (4) and the molar formulation (J mol^{-1}) for the chemical potentials in Fick's law (equation (5)). The way that kg and moles are mixed in the treatment of Tajčmanová et al. (2021) leads to contradictory results that contravene the dissipation inequality. In contrast, if consistent units are used, entropy production due to diffusion is always positive for both the molar (equation (7)) and barycentric formulations as expected (de Groot & Mazur, 1962; Gurtin et al., 2010). We note that this holds true for non-isothermal processes as well, as is described in standard texts.

Entropy production arguments alone, therefore, cannot be used to distinguish between the formulations. Instead, admissible formulations for modeling diffusion in crystalline solids must be the one(s) that satisfy the additional constraints imposed by the network model (Gurtin et al., 2010). The molar formulation is naturally consistent with these constraints (Brady, 1975; Howard & Lidiard, 1964). On the other hand, the unconstrained barycentric formulation, although perfectly appropriate for fluids, is not (Cahn & Larché, 1983). These differences lead to sharply contrasting results. For example, the barycentric approach employed without network constraints predicts that components

will stratify by density, meaning that components with high densities will preferentially diffuse toward high stress regions (e.g., in Fig. 4, almandine and spessartine would increase with applied stress while pyrope and grossular decrease). This is by analogy with fluids such as the atmosphere, which stratify by density in Earth’s gravity field owing to body forces (Tajčmanová et al., 2021). In contrast, the molar approach predicts that components with smaller molar volumes will diffuse toward high stress regions to reduce the strain energy arising from surface forces (Fig. 4), consistent with the Gorsky effect (Gorsky, 1935). These predicted behaviors are at strong variance, but ultimately provide testable predictions for future work.

7. Conclusions

Larché and Cahn (1973, 1978a, 1978b, 1982, 1985) offer a foundational basis for investigating the effects of stress on the thermodynamics of multi-component, elastic solids. In their work, they derive an equation that quantitatively links stresses to the compositions of multi-component solids. This equation, which we refer to as the Larché-Cahn equation (equation (2)), allows compositions to be calculated for solid solutions with any number of endmembers under arbitrary stress states. Intracrystalline diffusion is the mechanism by which stress-induced composition changes will take place. We show that diffusion following Larché-Cahn theory leads to negative free energy change and positive entropy production, as required for any real process. Thus, the Larché-Cahn theory is feasible for calculating stress-induced composition changes.

Powell et al. (2018) and Wheeler (2018) applied the Larché-Cahn equation to binary solid solutions assuming ideal mixing behavior. Their results indicated that hundreds of MPa to GPa stress variations were needed to alter mineral compositions by a few hundredths of a mole fraction. However, important aspects of solid solutions such as non-ideal behavior and additional endmembers were not considered.

Here, we have both incorporated non-ideal mixing behavior into the Larché-Cahn equation and extended its use beyond binary solid solutions. Our results show that non-ideal mixing behavior increases calculated stress-induced composition changes by up to an order of magnitude, depending on how near a solid solution is to a solvus. Consequently, stresses on the order of tens to a few hundred MPa may be all that is required to shift the composition of common metamorphic minerals (e.g., garnet, clinopyroxene, and plagioclase) by several hundredths of a mole fraction or more. Further, when additional endmembers are considered (e.g., the common Py–Alm–Grs–Sps garnet solid-solution), the calculated magnitude and sometimes even the direction of stress-induced composition change is altered relative to a binary calculation. For example, almandine would increase with applied stress in an Alm–Grs binary, but if pyrope is also considered, almandine would be predicted to decrease instead (Fig. 4). As such, a full treatment that considers non-ideal mixing behavior and all pertinent solid solution endmembers is required to model stress-induced composition changes.

It is entirely feasible that the Larché-Cahn equation can be used in reverse to infer stresses from preserved mineral compositions. Wheeler (2018) proposed in particular that crystallographic anisotropy can be exploited as anisotropic minerals will have different compositions as a function of orientation. Stress-induced composition changes are most likely to be observed in non-hydrostatically stressed rocks that were hot, dry, and composed of strong minerals. Therefore, we propose that pyroxenes and plagioclase in dry, lower crustal granulite facies rocks offer a promising environment to test and apply the Larché-Cahn equation to infer paleo stresses. There is presently great interest in the stress states that lower crustal granulites experience since the transition from strong, dry lower crust to weaker, hydrous lithologies is thought to be an important control on crustal rheology (e.g., Jamtveit et al., 2019; Menegon et al., 2021). Therefore, the Larché-Cahn equation offers exciting new prospects for determining the magnitudes of non-hydrostatic stress in vital lithospheric settings such as lower crustal granulites.

Acknowledgments

We thank H. Austrheim, M. T. Brandon, X. Chu, A. Haws, S. Piazzolo, and A. Putnis for thoughtful discussions, and R. Powell and an anonymous referee for their thorough and constructive reviews. In particular, R. Powell shared his insights regarding equilibrium under non-hydrostatic conditions, which are much appreciated. Financial support from the US National Science Foundation Directorate of Geosciences (EAR-2208229) and Yale University is gratefully acknowledged.

Open Research

The thermodynamic dataset is from Holland and Powell (2011). Data were not created for this research.

References

- Ague, J. J., & Axler, J. A. (2016). Interface coupled dissolution-precipitation in garnet from subducted granulites and ultrahigh-pressure rocks revealed by phosphorous, sodium, and titanium zonation. *American Mineralogist*, *101*(7), 1696-1699. <https://doi.org/10.2138/am-2016-5707>
- Altenberger, U., Prosser, G., Grande, A., Günter, C., & Langone, A. (2013). A seismogenic zone in the deep crust indicated by pseudotachylytes and ultramylonites in granulite-facies rocks of Calabria (Southern Italy). *Contributions to Mineralogy and Petrology*, *166*(4), 975-994. <https://doi.org/10.1007/s00410-013-0904-3>
- Alcantar, N., Israelachvili, J., & Boles, J. (2003). Forces and ionic transport between mica surfaces: Implications for pressure solution. *Geochimica*

- et Cosmochimica acta*, 67(7), 1289-1304. [https://doi.org/10.1016/S0016-7037\(02\)01270-X](https://doi.org/10.1016/S0016-7037(02)01270-X)
- Altree-Williams, A., Pring, A., Ngothai, Y., & Brugger, J. (2015). Textural and compositional complexities resulting from coupled dissolution–reprecipitation reactions in geomaterials. *Earth-Science Reviews*, 150, 628-651. <https://doi.org/10.1016/j.earscirev.2015.08.013>
- Austrheim, H. (1987). Eclogitization of lower crustal granulites by fluid migration through shear zones. *Earth and Planetary Science Letters*, 81(2-3), 221-232. [https://doi.org/10.1016/0012-821X\(87\)90158-0](https://doi.org/10.1016/0012-821X(87)90158-0)
- Austrheim, H. (2013). Fluid and deformation induced metamorphic processes around Moho beneath continent collision zones: Examples from the exposed root zone of the Caledonian mountain belt, W-Norway. *Tectonophysics*, 609, 620-635. <https://doi.org/10.1016/j.tecto.2013.08.030>
- Babeyko, A. Y., & Sobolev, S. V. (2008). High-resolution numerical modeling of stress distribution in visco-elasto-plastic subducting slabs. *Lithos*, 103(1-2), 205-216. <https://doi.org/10.1016/j.lithos.2007.09.015>
- Berman, R. G. (1990). Mixing properties of Ca-Mg-Fe-Mn garnets. *American Mineralogist*, 75(3-4), 328-344.
- Bernabé, Y., & Evans, B. (2014). Pressure solution creep of random packs of spheres. *Journal of Geophysical Research: Solid Earth*, 119(5), 4202-4218. <https://doi.org/10.1002/2014JB011036>
- Bower, A. F., Guduru, P. R., & Sethuraman, V. A. (2011). A finite strain model of stress, diffusion, plastic flow, and electrochemical reactions in a lithium-ion half-cell. *Journal of the Mechanics and Physics of Solids*, 59(4), 804-828. <https://doi.org/10.1016/j.jmps.2011.01.003>
- Brady, J. B. (1975). Reference frames and diffusion coefficients. *American Journal of Science*, 275(8), 954-983.
- Brown, J. M., Angel, R. J., & Ross, N. L. (2016). Elasticity of plagioclase feldspars. *Journal of Geophysical Research: Solid Earth*, 121, 663-675. <https://doi.org/10.1002/2015JB012736>
- Bruton, C. J., & Helgeson, H. C. (1983). Calculation of the chemical and thermodynamic consequences of differences between fluid and geostatic pressure in hydrothermal systems. *American Journal of Science*, 283A, 540-588.
- Burg, J. P., & Gerya, T. V. (2005). The role of viscous heating in Barrovian metamorphism of collisional orogens: thermomechanical models and application to the Lepontine Dome in the Central Alps. *Journal of Metamorphic Geology*, 23(2), 75-95. <https://doi.org/10.1111/j.1525-1314.2005.00563.x>
- Burov, E., & Yamato, P. (2008). Continental plate collision, P–T–t–z conditions and unstable vs. stable plate dynamics: insights from thermo-mechanical modelling. *Lithos*, 103(1-2), 178-204. <https://doi.org/10.1016/j.lithos.2007.09.014>

- Bystricky, M., & Mackwell, S. (2001). Creep of dry clinopyroxene aggregates. *Journal of Geophysical Research: Solid Earth*, *106*(B7), 13443-13454. <https://doi.org/10.1029/2001JB000333>
- Cahn, J. W., & Larche, F. C. (1983). An invariant formulation of multicomponent diffusion in crystals. *Scripta metallurgica*, *17*(7), 927-932. [https://doi.org/10.1016/0036-9748\(83\)90264-8](https://doi.org/10.1016/0036-9748(83)90264-8)
- Camacho, A., Vernon, R. H., & Gerald, J. F. (1995). Large volumes of anhydrous pseudotachylyte in the Woodroffe Thrust, eastern Musgrave Ranges, Australia. *Journal of Structural Geology*, *17*(3), 371-383. [https://doi.org/10.1016/0191-8141\(94\)00069-C](https://doi.org/10.1016/0191-8141(94)00069-C)
- Campbell, L. R., Menegon, L., Fagereng, Å., & Pennacchioni, G. (2020). Earthquake nucleation in the lower crust by local stress amplification. *Nature communications*, *11*(1), 1-9. <https://doi.org/10.1038/s41467-020-15150-x>
- Centrella, S., Austrheim, H., & Putnis, A. (2015). Coupled mass transfer through a fluid phase and volume preservation during the hydration of granulite: An example from the Bergen Arcs, Norway. *Lithos*, *236*, 245-255. <https://doi.org/10.1016/j.lithos.2015.09.010>
- Chu, X., Ague, J. J., Podladchikov, Y. Y., & Tian, M. (2017). Ultrafast eclogite formation via melting-induced overpressure. *Earth and Planetary Science Letters*, *479*, 1-17. <https://doi.org/10.1016/j.epsl.2017.09.007>
- Connolly, J. A. D. (2009). The geodynamic equation of state: What and how. *Geochemistry Geophysics, Geosystems*, *10*, Q10014. <https://doi.org/10.1029/2009GC002540>
- Cui, Z., Gao, F., & Qu, J. (2012). A finite deformation stress-dependent chemical potential and its applications to lithium ion batteries. *Journal of the Mechanics and Physics of Solids*, *60*(7), 1280-1295. <https://doi.org/10.1016/j.jmps.2012.03.008>
- Dahlen, F. A., (1992). Metamorphism of nonhydrostatically stressed rocks. *American Journal of Science*, *292*, 184-198. <https://doi.org/10.2475/ajs.292.3.184>
- De Groot, S. R., & Mazur, P. (1962). *Non-Equilibrium Thermodynamics*. Dover, New York.
- Dimanov, A., Dresen, G., Xiao, X., & Wirth, R. (1999). Grain boundary diffusion creep of synthetic anorthite aggregates: The effect of water. *Journal of Geophysical Research: Solid Earth*, *104*(B5), 10483-10497. <https://doi.org/10.1029/1998JB900113>
- Engvik, A. K., Golla-Schindler, U., Berndt, J., Austrheim, H., & Putnis, A. (2009). Intragranular replacement of chlorapatite by hydroxy-fluor-apatite during metasomatism. *Lithos*, *112*(3-4), 236-246. <https://doi.org/10.1016/j.lithos.2009.02.005>
- Evans, K. A., & Powell, R. (2015). The effect of subduction on the sulfur, carbon, and redox budget of lithospheric mantle. *Journal of Metamorphic Geology*, *33*, 649-670. <https://doi.org/10.1111/jmg.12140>

- Fukai, Y., & Sugimoto, H. (1985). Diffusion of hydrogen in metals. *Advances in Physics*, 34(2), 263-326. <https://doi.org/10.1080/00018738500101751>
- Ganguly, J., Cheng, W., & Tirone, M. (1996). Thermodynamics of aluminosilicate garnet solid solution: new experimental data, an optimized model, and thermometric applications. *Contributions to Mineralogy and Petrology*, 126(1), 137-151. <https://doi.org/10.1007/s004100050240>
- Geisler, T., Schaltegger, U., & Tomaschek, F. (2007). Re-equilibration of zircon in aqueous fluids and melts. *Elements*, 3(1), 43-50. <https://doi.org/10.2113/gselements.3.1.43>
- Gerya, T. (2015). Tectonic overpressure and underpressure in lithospheric tectonics and metamorphism. *Journal of Metamorphic Geology*, 33(8), 785-800. <https://doi.org/10.1111/jmg.12144>
- Gibbs, J. W. (1878). On the equilibrium of heterogeneous substances. *Connecticut Academy of Arts and Sciences Transactions*, 3, 343-524.
- Gorsky, W. S. (1935). Theorie der elastischen Nachwirkung in ungeordneten Mischkristallen (elastische Nachwirkung zweiter Art). *Physikalische Zeitschrift der Sowjetunion*, 88, 457-471.
- Gratier, J. P. (1987). Pressure solution-deposition creep and associated tectonic differentiation in sedimentary rocks. *Geological Society, London, Special Publications*, 29(1), 25-38. <https://doi.org/10.1144/GSL.SP.1987.029.01.03>
- Gratier, J. P., Dysthe, D. K., & Renard, F. (2013). The role of pressure solution creep in the ductility of the Earth's upper crust. *Advances in geophysics*, 54, 47-179. <https://doi.org/10.1016/B978-0-12-380940-7.00002-0>
- Green, E. C. R., White, R. W., Diener, J. F. A., Powell, R., Holland, T. J. B., & Palin, R. M. (2016). Activity-composition relations for the calculation of partial melting equilibria in metabasic rocks. *Journal of Metamorphic Geology*, 34, 845-869. <https://doi.org/10.1111/jmg.12211>
- Green, H. W. (1980). On the thermodynamics of non-hydrostatically stressed solids. *Philosophical Magazine A*, 41, 637-647. <https://doi.org/10.1080/01418618008239339>
- Gurtin, M. E., Fried, E., & Anand, L. (2010). *The mechanics and thermodynamics of continua*. Cambridge University Press.
- Guyer, J. E., & Voorhees, P. W. (1996). Morphological stability of alloy thin films. *Physical Review B*, 54(16), 11710. <https://doi.org/10.1103/PhysRevB.54.11710>
- Harlov, D. E., Wirth, R., & Hetherington, C. J. (2011). Fluid-mediated partial alteration in monazite: the role of coupled dissolution-precipitation in element redistribution and mass transfer. *Contributions to Mineralogy and Petrology*, 162(2), 329-348. <https://doi.org/10.1007/s00410-010-0599-7>
- Hess, B. L., & Ague, J. J. (2021). Quantifying the Effects of Non-hydrostatic Stress on Single-component Polymorphs. *Journal of Geophysical Research: Solid Earth*, 126, e2020JB021594. <https://doi.org/10.1029/2020JB021594>

- Hobbs, B. E., & Ord, A. (2016). Does non-hydrostatic stress influence the equilibrium of metamorphic reactions? *Earth-Science Reviews*, *163*, 190-233. <https://doi.org/10.1016/j.earscirev.2016.08.013>
- Hobbs, B. E., & Ord, A. (2017). Pressure and equilibrium in deforming rocks. *Journal of Metamorphic Geology*, *35*, 967-982. <https://doi.org/10.1111/jmg.12263>
- Holland, T. J. B., & Powell, R. (2011). An improved and extended internally consistent thermodynamic dataset for phases of petrological interest, involving a new equation of state for solids. *Journal of Metamorphic Geology*, *29*, 333-383. <https://doi.org/10.1111/j.1525-1314.2010.00923.x>
- Holland, T. J. B., Green, E. C. R., & Powell, R. (2021). A thermodynamic model for feldspars in KAlSi_3O_8 – $\text{NaAlSi}_3\text{O}_8$ – $\text{CaAl}_2\text{Si}_2\text{O}_8$ for mineral equilibrium calculations. *Journal of Metamorphic Geology*, *40*, 1-14. <https://doi.org/10.1111/jmg.12639>
- Holland, T. J. B., Hudson, N. F. C., Powell, R., & Harte, B. (2013). New thermodynamic models and calculated phase equilibria in NCF-MAS for basic and ultrabasic compositions through the transition zone into the uppermost lower mantle. *Journal of Petrology*, *54*(9), 1901-1920. <https://doi.org/10.1093/petrology/egt035>
- Holland, T., & Powell, R. (2003). Activity–composition relations for phases in petrological calculations: an asymmetric multicomponent formulation. *Contributions to Mineralogy and Petrology*, *145*(4), 492-501. <https://doi.org/10.1007/s00410-003-0464-z>
- Howard, R. E., & Lidiard, A. B. (1964). Matter transport in solids. *Reports on progress in Physics*, *27*(1), 161.
- Jamtveit, B., Petley-Ragan, A., Incel, S., Dunkel, K. G., Aupart, C., Austrheim, H., et al, (2019). The effects of earthquakes and fluids on the metamorphism of the lower continental crust. *Journal of Geophysical Research: Solid Earth*, *124*(8), 7725-7755. <https://doi.org/10.1029/2018JB016461>
- Kamachali, R. D., Borukhovich, E., Hatcher, N., & Steinbach, I. (2014). DFT-supported phase-field study on the effect of mechanically driven fluxes in Ni_4Ti_3 precipitation. *Modelling and Simulation in Materials Science and Engineering*, *22*(3), 034003.
- Kamachali, R. D., Schwarze, C., Lin, M., Diehl, M., Shanthraj, P., Prahl, U., et al. (2018). Numerical benchmark of phase-field simulations with elastic strains: precipitation in the presence of chemo-mechanical coupling. *Computational Materials Science*, *155*, 541-553. <https://doi.org/10.1016/j.commatsci.2018.09.011>
- Kamb, W. B. (1959). Theory of preferred crystal orientation developed by crystallization under stress. *The Journal of Geology*, *67*, 153-170. <https://doi.org/10.1086/626571>

- Kamb, W. B. (1961). The thermodynamic theory of nonhydrostatically stressed solids. *Journal of Geophysical Research*, *66*, 259-271. <https://doi.org/10.1029/JZ066i001p00259>
- Karato, S. I., Wang, Z., Liu, B., & Fujino, K. (1995). Plastic deformation of garnets: systematics and implications for the rheology of the mantle transition zone. *Earth and Planetary Science Letters*, *130*(1-4), 13-30. [https://doi.org/10.1016/0012-821X\(94\)00255-W](https://doi.org/10.1016/0012-821X(94)00255-W)
- Keller, D. S., & Ague, J. J. (2018). High-pressure granulite facies metamorphism (1.8 GPa) revealed in silica-undersaturated garnet-spinel-corundum gneiss, Central Maine Terrane, Connecticut, USA. *American Mineralogist*, *103*(11), 1851-1868. <https://doi.org/10.2138/am-2018-6543>
- Kerrick, D. M., & Connolly, J. A. D. (2001). Metamorphic devolatilization of subducted marine sediments and the transport of volatiles into the Earth's mantle. *Nature*, *411*, 293-296. <https://doi.org/10.1038/35077056>
- King, K. C., Voorhees, P. W., Olson, G. B., & Mura, T. (1991). Solute distribution around a coherent precipitate in a multicomponent alloy. *Metallurgical Transactions A*, *22*, 2199-2210. <https://doi.org/10.1007/BF02664986>
- Larché, F., & Cahn, J. W. (1973). A linear theory of thermochemical equilibrium of solids under stress. *Acta Metallurgica*, *21*, 1051-1063. [https://doi.org/10.1016/0001-6160\(73\)90021-7](https://doi.org/10.1016/0001-6160(73)90021-7)
- Larché, F., & Cahn, J. W. (1978a). A nonlinear theory of thermochemical equilibrium of solids under stress. *Acta Metallurgica*, *26*, 53-60. [https://doi.org/10.1016/0001-6160\(78\)90201-8](https://doi.org/10.1016/0001-6160(78)90201-8)
- Larché, F., & Cahn, J. W. (1978b). Thermochemical equilibrium of multiphase solids under stress. *Acta Metallurgica*, *26*, 1579-1589. [https://doi.org/10.1016/0001-6160\(78\)90067-6](https://doi.org/10.1016/0001-6160(78)90067-6)
- Larché, F., & Cahn, J. W. (1982). The effect of self-stress on diffusion in solids. *Acta Metallurgica*, *30*, 1835-1845. [https://doi.org/10.1016/0001-6160\(82\)90023-2](https://doi.org/10.1016/0001-6160(82)90023-2)
- Larché, F., & Cahn, J. W. (1985). Overview no. 41 The interactions of composition and stress in crystalline solids. *Acta Metallurgica*, *33*, 331-357. [https://doi.org/10.1016/0001-6160\(85\)90077-X](https://doi.org/10.1016/0001-6160(85)90077-X)
- Lehner, F. K. (1990). Thermodynamics of rock deformation by pressure solution. In *Deformation processes in minerals, ceramics and rocks* (pp. 296-333). Springer, Dordrecht.
- Li, L., Long, H., Raterron, P., & Weidner, D. (2006). Plastic flow of pyrope at mantle pressure and temperature. *American Mineralogist*, *91*(4), 517-525. <https://doi.org/10.2138/am.2006.1913>
- Li, J. L., Schwarzenbach, E. M., John, T., Ague, J. J., Huang, F., Gao, J., et al. (2020). Uncovering and quantifying the subduction zone sul-

- fur cycle from the slab perspective. *Nature Communications*, *11*, 1-12. <https://doi.org/10.1038/s41467-019-14110-4>
- Li, Z. H., Gerya, T. V., & Burg, J. P. (2010). Influence of tectonic overpressure on P-T paths of HP–UHP rocks in continental collision zones: thermomechanical modelling. *Journal of Metamorphic Geology*, *28*, 227–247. <https://doi.org/10.1111/j.1525-1314.2009.00864.x>
- Lian, S., Zhou, M. M., Yan, Y., Terblans, J. J., Swart, H. C., Wang, J., & Xu, C. (2021). Equilibrium segregation in the stressed Ni(111)(Au) nano-films on inert substrate. *Journal of Materials Science*, *56*(10), 6217-6226. <https://doi.org/10.1007/s10853-020-05632-0>
- MacDonald, G. J. (1957). Thermodynamics of solids under non-hydrostatic stress with geologic applications. *American Journal of Science*, *255*, 266-281. <https://doi.org/10.2475/ajs.255.4.266>
- MacDonald, G. J. (1960). Orientation of anisotropic minerals in a stress field. *Geological Society of America Memoirs*, *79*, 1-8.
- Meca, E., Münch, A., & Wagner, B. (2016). Thin-film electrodes for high-capacity lithium-ion batteries: influence of phase transformations on stress. *Proceedings of the Royal Society A: Mathematical, Physical and Engineering Sciences*, *472*(2193), 20160093. <https://doi.org/10.1098/rspa.2016.0093>
- Mei, S., Suzuki, A. M., Kohlstedt, D. L., & Xu, L. (2010). Experimental investigation of the creep behavior of garnet at high temperatures and pressures. *Journal of Earth Science*, *21*(5), 532-540. <https://doi.org/10.1007/s12583-010-0127-8>
- Menegon, L., Campbell, L., Mancktelow, N., Camacho, A., Wex, S., Papa, S., et al. (2021). The earthquake cycle in the dry lower continental crust: insights from two deeply exhumed terranes (Musgrave Ranges, Australia and Lofoten, Norway). *Philosophical transactions of the Royal Society A*, *379*(2193), 20190416. <https://doi.org/10.1098/rsta.2019.0416>
- Molnar, P., England, P., & Martinod, J. (1993). Mantle dynamics, uplift of the Tibetan Plateau, and the Indian monsoon. *Reviews of Geophysics*, *31*, 357-396. <https://doi.org/10.1029/93RG02030>
- Moulas, E., Schmalholz, S. M., Podladchikov, Y., Tajčmanová, L., Kostopoulos, D., & Baumgartner, L. (2019a). Relation between mean stress, thermodynamic, and lithostatic pressure. *Journal of metamorphic geology*, *37*, 1-14. <https://doi.org/10.1111/jmg.12446>
- Moulas, E., Sokoutis, D., & Willingshofer, E. (2019b). Pressure build-up and stress variations within the Earth's crust in the light of analogue models. *Scientific reports*, *9*, 1-8. <https://doi.org/10.1038/s41598-018-38256-1>
- Müller, T., Massonne, H. J., & Willner, A. P. (2015). Timescales of exhumation and cooling inferred by kinetic modeling: An example using a lamellar garnet

- pyroxenite from the Variscan Granulitgebirge, Germany. *American Mineralogist*, 100(4), 747-759. <https://doi.org/10.2138/am-2015-4946>
- Myung, I. J. (2003). Tutorial on maximum likelihood estimation. *Journal of mathematical Psychology*, 47(1), 90-100. [https://doi.org/10.1016/S0022-2496\(02\)00028-7](https://doi.org/10.1016/S0022-2496(02)00028-7)
- Orlandini, O. F., Mahan, K. H., Williams, M. J., Regan, S. P., & Mueller, K. J. (2019). Evidence for deep crustal seismic rupture in a granulite-facies, intraplate, strike-slip shear zone, northern Saskatchewan, Canada. *Bulletin*, 131(3-4), 403-425. <https://doi.org/10.1130/B31922.1>
- Pálsson, G. K., Bliersbach, A., Wolff, M., Zamani, A., & Hjörvarsson, B. (2012). Using light transmission to watch hydrogen diffuse. *Nature communications*, 3, 892. <https://doi.org/10.1038/ncomms1897>
- Paterson, M. S. (1973). Nonhydrostatic thermodynamics and its geological applications. *Reviews of Geophysics and Space Physics*, 11, 355-389.
- Petley-Ragan, A., Dunkel, K. G., Austrheim, H., Ildefonse, B., & Jamtveit, B. (2018). Microstructural records of earthquakes in the lower crust and associated fluid-driven metamorphism in plagioclase-rich granulites. *Journal of Geophysical Research: Solid Earth*, 123(5), 3729-3746. <https://doi.org/10.1029/2017JB015348>
- Plümper, O., & Putnis, A. (2009). The complex hydrothermal history of granitic rocks: multiple feldspar replacement reactions under subsolidus conditions. *Journal of Petrology*, 50(5), 967-987. <https://doi.org/10.1093/petrology/egp028>
- Poli, S., & Schmidt, M. (2002). Petrology of Subducted Slabs. *Annual Reviews in Earth and Planetary Sciences*, 30, 207-235. <https://doi.org/10.1146/annurev.earth.30.091201.140550>
- Powell, R., Evans, K. A., Green, E. C. R., & White, R. W. (2018). On equilibrium in non-hydrostatic metamorphic systems. *Journal of Metamorphic Geology*, 36, 419-438. <https://doi.org/10.1111/jmg.12298>
- Powell, R., Evans, K. A., Green, E. C., & White, R. W. (2019). The truth and beauty of chemical potentials. *Journal of Metamorphic Geology*, 37(7), 1007-1019. <https://doi.org/10.1111/jmg.12484>
- Putnis, A. (2002). Mineral replacement reactions: from macroscopic observations to microscopic mechanisms. *Mineralogical Magazine*, 66(5), 689-708. <https://doi.org/10.1180/0026461026650056>
- Putnis, A., & Austrheim, H. (2010). Fluid-induced processes: metasomatism and metamorphism. *Geofluids*, 10(1-2), 254-269. <https://doi.org/10.1111/j.1468-8123.2010.00285.x>
- Putnis, A., Jamtveit, B., & Austrheim, H. (2017). Metamorphic processes and seismicity: the Bergen Arcs as a natural laboratory. *Journal of Petrology*, 58(10), 1871-1898. <https://doi.org/10.1093/petrology/egx076>

- Putnis, A., & John, T. (2010). Replacement processes in the Earth's crust. *Elements*, 6(3), 159-164. <https://doi.org/10.2113/gselements.6.3.159>
- Regan, S. P., Williams, M. L., Leslie, S., Mahan, K. H., Jercinovic, M. J., & Holland, M. E. (2014). The Cora Lake shear zone, Athabasca granulite terrane, an intraplate response to far-field orogenic processes during the amalgamation of Laurentia. *Canadian Journal of Earth Sciences*, 51(9), 877-901. <https://doi.org/10.1139/cjes-2014-0015>
- Robin, P. F. (1978). Pressure solution at grain-to-grain contacts. *Geochimica et Cosmochimica Acta*, 49, 1383-1389. [https://doi.org/10.1016/0016-7037\(78\)90043-1](https://doi.org/10.1016/0016-7037(78)90043-1)
- Rubatto, D., Müntener, O., Barnhoorn, A., & Gregory, C. (2008). Dissolution-reprecipitation of zircon at low-temperature, high-pressure conditions (Lanzo Massif, Italy). *American Mineralogist*, 93(10), 1519-1529. <https://doi.org/10.2138/am.2008.2874>
- Rutter, E. H. (1983). Pressure solution in nature, theory and experiment. *Journal of the Geological Society*, 140(5), 725-740. <https://doi.org/10.1144/gsjgs.140.5.0725>
- Rybacki, E., & Dresen, G. (2004). Deformation mechanism maps for feldspar rocks. *Tectonophysics*, 382(3-4), 173-187. <https://doi.org/10.1016/j.tecto.2004.01.006>
- Schaumann, G., Völkl, J., & Alefeld, G. (1968). Relaxation process due to long-range diffusion of hydrogen and deuterium in niobium. *Physical Review Letters*, 21(13), 891. <https://doi.org/10.1103/PhysRevLett.21.891>
- Schaumann, G., Völkl, J., & Alefeld, G. (1970). The diffusion coefficients of hydrogen and deuterium in vanadium, niobium, and tantalum by gorsky-effect measurements. *physica status solidi (b)*, 42(1), 401-413. <https://doi.org/10.1002/pssb.19700420141>
- Schmalholz, S. M., Medvedev, S., Lechmann, S. M., & Podladchikov, Y. (2014a). Relationship between tectonic overpressure, deviatoric stress, driving force, isostasy and gravitational potential energy. *Geophysical Journal International*, 197, 680-696. <https://doi.org/10.1093/gji/ggu040>
- Schmalholz, S. M., Duretz, T., Schenker, F. L., & Podladchikov, Y. Y. (2014b). Kinematics and dynamics of tectonic nappes: 2-D numerical modelling and implications for high and ultra-high pressure tectonism in the Western Alps. *Tectonophysics*, 631, 160-175. <https://doi.org/10.1016/j.tecto.2014.05.018>
- Schwarze, C., Gupta, A., Hickel, T., & Kamachali, R. D. (2017). Phase-field study of ripening and rearrangement of precipitates under chemomechanical coupling. *Physical Review B*, 95(17), 174101. <https://doi.org/10.1103/PhysRevB.95.174101>
- Sethuraman, V. A., Srinivasan, V., Bower, A. F., & Guduru, P. R. (2010). In situ measurements of stress-potential coupling in lithiated silicon. *Journal of the Electrochemical Society*, 157, A1253. <https://doi.org/10.1149/1.3489378>

- Shi, S., Markmann, J., & Weissmüller, J. (2018). Verifying Larché-Cahn elasticity, a milestone of 20th-century thermodynamics. *Proceedings of the National Academy of Sciences*, *115*, 10914-10919. <https://doi.org/10.1073/pnas.1809355115>
- Smit, M. A., Scherer, E. E., John, T., & Janssen, A. (2011). Creep of garnet in eclogite: Mechanisms and implications. *Earth and Planetary Science Letters*, *311*(3-4), 411-419. <https://doi.org/10.1016/j.epsl.2011.09.024>
- Spencer, B. J., Voorhees, P. W., & Davis, S. H. (1991). Morphological instability in epitaxially strained dislocation-free solid films. *Physical review letters*, *67*(26), 3696. <https://doi.org/10.1103/PhysRevLett.67.3696>
- Stewart, E. M., & Ague, J. J. (2018). Infiltration-driven metamorphism, New England, USA: Regional CO₂ fluxes and implications for Devonian climate and extinctions. *Earth and Planetary Science Letters*, *489*, 123-134. <https://doi.org/10.1016/j.epsl.2018.02.028>
- Stüwe, K., & Sandiford, M. (1994). Contribution of deviatoric stresses to metamorphic P-T paths: an example appropriate to low-P, high-T metamorphism. *Journal of Metamorphic Geology*, *12*(4), 445-454. <https://doi.org/10.1111/j.1525-1314.1994.tb00034.x>
- Tajčmanová, L., Podladchikov, Y., Moulas, E., & Khakimova, L. (2021). The choice of a thermodynamic formulation dramatically affects modelled chemical zoning in minerals. *Scientific Reports*, *11*, 18740. <https://doi.org/10.1038/s41598-021-97568-x>
- Tajčmanová, L., Podladchikov, Y., Powell, R., Moulas, E., Vrijmoed, J. C., & Connolly, J. A. D. (2014). Grain-scale pressure variations and chemical equilibrium in high-grade metamorphic rocks. *Journal of Metamorphic Geology*, *32*, 195-207. <https://doi.org/10.1111/jmg.12066>
- Tajčmanová, L., Vrijmoed, J., & Moulas, E. (2015). Grain-scale pressure variations in metamorphic rocks: implications for the interpretation of petrographic observations. *Lithos*, *216*, 338-351. <https://doi.org/10.1016/j.lithos.2015.01.006>
- Verhoogen, J. (1951). The chemical potential of a stressed solid. *Eos, Transactions American Geophysical Union*, *32*, 251-258. <https://doi.org/10.1029/TR032i002p00251>
- Völkl, J. (1972). The gorsky effect. *Berichte der Bunsengesellschaft für physikalische Chemie*, *76*(8), 797-805. <https://doi.org/10.1002/bbpc.19720760834>
- Voorhees, P. W., & Johnson, W. C. (1989). The thermodynamics of a coherent interface. *The Journal of Chemical Physics*, *90*(5), 2793-2801. <https://doi.org/10.1063/1.455928>
- Voorhees, P. W., & Johnson, W. C. (2004). The thermodynamics of elastically stressed crystals. *Solid State Physics-Advances in Research and Applications*, *59*, 1-201. [https://doi.org/10.1016/S0081-1947\(04\)80003-1](https://doi.org/10.1016/S0081-1947(04)80003-1)
- Vrijmoed, J. C., & Podladchikov, Y. Y. (2015). Thermodynamic equilibrium at heterogeneous pressure. *Contributions to Mineralogy and Petrology*, *170*(1),

1-27. <https://doi.org/10.1007/s00410-015-1156-1>

Wang, Z., & Ji, S. (1999). Deformation of silicate garnets: Brittle-ductile transition and its geological implications. *Canadian Mineralogist*, *37*, 525-541.

Wang, R. V., Stephenson, G. B., Fong, D. D., Jiang, F., Fuoss, P. H., Eastman, J. A., et al. (2006). Real time x-ray observation of lattice pulling during growth of epitaxial Pb(Zr,Ti)O₃ films. *Applied physics letters*, *89*(22), 221914. <https://doi.org/10.1063/1.2387980>

Wheeler, J. (2014). Dramatic effects of stress on metamorphic reactions. *Geology*, *42*, 647-650. <https://doi.org/10.1130/G35718.1>

Wheeler, J. (2018). The effects of stress on reactions in the Earth: Sometimes rather mean, usually normal, always important. *Journal of Metamorphic Geology*, *36*, 439-461. <https://doi.org/10.1111/jmg.12299>

Wheeler, J. (2020). A unifying basis for the interplay of stress and chemical processes in the Earth: support from diverse experiments. *Contributions to Mineralogy and Petrology*, *175*, 1-27. <https://doi.org/10.1007/s00410-020-01750-9>

White, R. W., Powell, R., & Johnson, T. E. (2014). The effect of Mn on mineral stability in metapelites revisited: new a-x relations for manganese-bearing minerals. *Journal of Metamorphic Geology*, *32*(8), 809-828. <https://doi.org/10.1111/jmg.12095>

Wintsch, R. P., & Yi, K. (2002). Dissolution and replacement creep: a significant deformation mechanism in mid-crustal rocks. *Journal of Structural Geology*, *24*(6-7), 1179-1193. [https://doi.org/10.1016/S0191-8141\(01\)00100-6](https://doi.org/10.1016/S0191-8141(01)00100-6)

Zhang, J., & Green, H. W. (2007). Experimental investigation of eclogite rheology and its fabrics at high temperature and pressure. *Journal of Metamorphic Geology*, *25*, 97-115. <https://doi.org/10.1111/j.1525-1314.2006.00684.x>

Zhao, Y., Von Dreele, R. B., Shankland, T. J., Weidner, D. J., Zhang, J., Wang, Y., & Gasparik, T. (1997). Thermoelastic equation of state of jadeite NaAlSi₂O₆: An energy-dispersive Reitveld Refinement Study of low symmetry and multiple phases diffraction. *Geophysical Research Letters*, *24*, 5-8. <https://doi.org/10.1029/96GL03769>

Zhao, Y., Von Dreele, R. B., Zhang, J. Z., & Weidner, D. J. (1998). Thermoelastic equation of state of monoclinic pyroxene: CaMgSi₂O₆ diopside. *The Review of High Pressure Science and Technology*, *7*, 25-27. <https://doi.org/10.4131/jshpreview.7.25>

Zuza, A. V., Levy, D. A., & Mulligan, S. R. (2020). Geologic field evidence for non-lithostatic overpressure recorded in the North American Cordillera hinterland, northeast Nevada. *Geoscience Frontiers*, 101099. <https://doi.org/10.1016/j.gsf.2>

Figure 1. The network model. a) A generic crystal lattice where all the sites are filled by either yellow or blue atoms or vacancies (v). The lattice sites are independent of which species occupy the sites. b) The movement of one species is always coupled to the movement of another to conserve the lattice sites. Even though a vacancy is the absence of an atom on a site, that absence still adds energy to the system and so can be effectively treated as a species with a defined energy and position. The relative chemical potential quantifies the change in energy resulting from the coupled exchange of any two species on a given lattice site. c) Final state after exchanges have occurred. The total number of lattice sites and species are preserved.

Figure 2. Conceptual example of stress-induced composition change in a garnet. a) Garnet comprising 0.8 mole fraction pyrope (X_{Py}) and 0.2 mole fraction grossular (X_{Grs}) at equilibrium with a chemical reservoir that fixes the relative chemical potential at 1 GPa and 600 °C. b) A uniaxial stress is uniformly applied to the entire garnet, increasing the strain energy. The garnet is no longer in equilibrium with the surroundings. c) Garnet reduces its strain energy by exchanging the larger Ca^{2+} cation for the smaller Mg^{2+} cation. The exchange also increases the chemical energy of the garnet in the process. d) The diffusive exchange of Ca^{2+} for Mg^{2+} continues until the decrease in strain energy in the garnet from making the exchange is equal to the increase in chemical energy. At this point, the garnet is once more in equilibrium with the surrounding chemical reservoir as the total energy of the garnet cannot be reduced further via composition change. For a final applied stress of -0.5 GPa (negative stress is compressive), the composition is $X_{\text{Py}} = 0.851$ and $X_{\text{Grs}} = 0.149$. Figure designed after Voorhees and Johnson (2004) figure 16.

Figure 3. Composition change in solid solution binaries for given applied stresses at a fixed relative chemical potential from a reference pressure of 1 GPa. Part (a) uses ideal activity models whereas (b) incorporates non-ideal activity models for pyrope–almandine (Py–Alm) and pyrope–grossular (Py–Grs) garnet (Grt), jadeite–diopside (Jd–Di) clinopyroxene (Cpx), and anorthite–albite (An–Ab) plagioclase (Plag) feldspar. The composition change is shown for the former member of each solid solution (e.g., pyrope in Py–Alm). Results are given for all three crystallographic axes of clinopyroxene and plagioclase. There is only one result for each garnet binary as garnet is structurally isotropic. The calculations use 600 °C for garnet and plagioclase and 750 °C for clinopyroxene. Activity models: garnet, White et al. (2014); clinopyroxene, Green et al. (2016); plagioclase, Holland et al. (2003). Lattice parameters for garnet are from Holland and Powell (2011) using their equation of state at the given reference P and T . Lattice parameters for clinopyroxene are from Zhao et al. (1997, 1998) using their experimental data at 1.36 GPa and 600 °C. Lattice parameters for plagioclase are from Brown et al. (2016) at room P and T . Initial compositions are $X_{\text{Py}} = 0.5$ for Py–Alm, $X_{\text{Py}} = 0.75$ for Py–Grs, $X_{\text{Jd}} = 0.37$ for Jd–Di, and $X_{\text{An}} = 0.62$ for An–Ab.

Figure 4. Composition change with applied stress in a quaternary garnet solid

solution. The equilibrium composition of a garnet with pyrope–almandine–grossular–spessartine (Py–Alm–Grs–Sps) solid solution is plotted against applied uniaxial stress where negative stress is compressive and positive stress is extensional. The reference pressure and temperature are 1 GPa and 600 °C, and the initial composition is $X_{\text{Py}} = X_{\text{Alm}} = 0.45$ and $X_{\text{Grs}} = X_{\text{Sps}} = 0.05$. The activity model is from White et al. (2014). The lattice parameters are from the Holland and Powell (2011) dataset using their equation of state at the reference pressure and temperature.